Petroleum Science 20 (2023) 611–618

Contents lists available at ScienceDirect

Petroleum Science

journal homepage: www.keaipublishing.com/en/journals/petroleum-science

Original Paper

The deposition of asphaltenes under high-temperature and high-pressure (HTHP) conditions

Rui-Ying Xiong [a], Ji-Xiang Guo [a, *], Wyclif Kiyingi [a], Hai-Xia Xu [b], Xin-Peng Wu [a]

[a] Unconventional Petroleum Research Institute, China University of Petroleum, Beijing, 102249, China
[b] Petroleum Engineering Research Institute of Tarim Oilfield, China National Petroleum Corporation, Xinjiang, 84100, China

ARTICLE INFO

Article history:
Received 3 December 2021
Received in revised form
24 May 2022
Accepted 23 August 2022
Available online 8 September 2022

Edited by Jia-Jia Fei

Keywords:
HTHP reservoir
Asphaltene
Aggregation
Gas-oil ratio
HTHP PVT cell
Back-scattered light

ABSTRACT

In this work, the factors affecting asphaltenes deposition in high-temperature and high-pressure wells were studied using backscattered light and PVT equipment customized to suit the well conditions. In an examination of the intensity of backscattered light, it was revealed that there exists a linear relationship between temperature and asphaltene precipitation within a specific temperature range. Within this range, a decrease in temperature tends to accelerate asphaltene precipitation. However, the impacts of pressure and gas-oil ratio are more pronounced. The pressure depletion induces the asphaltenes to precipitate out of the solution, followed by the formation of flocs below the bubble point. In addition, an increase in the gas-oil ratio causes a more severe asphaltene deposition, shifting the location of asphaltenes to deep well sections.

1. Introduction

Asphaltene is one of the components of crude oil along with saturates, aromatics and resins-collectively referred to as SARA components. One of the distinguishing features of asphaltenes is that they are insoluble in *n*-alkanes but soluble in toluene. The asphaltene molecule has a complex molecular structure, high molecular weight, and strong polarity (Yao et al., 2020; Xiong et al., 2020a). It has been reported that the asphaltene molecule is composed of one or two polycyclic aromatic hydrocarbons (PAHs) (Dutta Majumdar et al., 2016). According to the classical colloidal model (Mousavi et al., 2016; Balestrin et al., 2017), the asphaltene is in the core of the micelle, surrounded by resins and aromatic molecules (Yarranton, 2005). The Yen-Mullins model is used extensively to describe the aggregation and formation of asphaltene Nano-colloidal compounds (Mullins, 2010; Mullins et al., 2012). With respect to the structure, considerable efforts have been made to understand the structure of asphaltenes (Schuler et al., 2015). It has been determined that the asphaltenes possess either the island or aryl-linked core molecular structure but not the archipelago structure as proposed in earlier studies. During the crude oil production process, the colloidal stability of crude oil is fragile and easily affected by temperature, pressure, solution gas content, and other factors (Zuo et al., 2012; Zuo et al., 2017; Guzmán et al., 2017, 2020; Xiong et al., 2020b). These factors directly affect the crude oil colloidal system and lead to precipitation, flocculation, aggregation, and deposition (Mohammed et al., 2020). The precipitated asphaltene tends to stick on the rock's surface, altering its wettability and reducing oil recovery (Alqam et al., 2021; Wang et al., 2021). Asphaltenes deposited on wellbore or facilities can also cause plugging (Lei et al., 2016; Ghadimi et al., 2019). This issue affects the efficiency of oil production and drives extra costs, i.e., removal of asphaltene plugging.

Currently, the method for assessing the stability of crude oil and its relationship with different factors remains a difficult task (Hemmati-Sarapardeh et al., 2019; Xiong et al., 2020b; Fakher et al., 2020; Raljević et al., 2021). Significant efforts have been made to understand and address this challenge. Studies have shown that the equilibrium state of crude oil with respect to the SARA fractions has a contributory role in the stability of crude oil with regard to forming colloids (Sinnathamb and Nor, 2012; Ashoori et al., 2017). Moreover, based on the colloidal instability index (CII), crude oil

* Corresponding author.
E-mail address: guojx003@126.com (J.-X. Guo).

https://doi.org/10.1016/j.petsci.2022.08.026

with a high resin-aromatic content is less prone to asphaltene risk compared to the one with a low range, Eq. (1) (Siddiqui et al., 2019; Nguele et al., 2022).

$$CII = \frac{Saturates + Asphaltenes}{Aromatics + Resins} \tag{1}$$

Besides, during oil production, the influence of temperature and pressure cannot be neglected. Generally, research on the effect of temperature on asphaltene precipitation is somewhat inconclusive. Temperature impact on asphaltene precipitation is linked to its influence on the solution density and entropy of the system (Hu and Guo, 2001; Bahrami et al., 2015). Thus, asphaltene precipitation and deposition may increase or decrease depending on the nature of the crude oil (kinetics), but the formation of asphaltene clusters is driven by entropy (Goual et al., 2014; Shojaei et al., 2020). In one study by Yudin and Anisimov and in a more recent one by Sullivan et al., attempts were made to clarify this issue. The asphaltenes aggregation and deposition kinetics were categorized as diffusion-limited aggregation and reaction-driven (limited reaction aggregation) (Yudin and Anisimov, 2007; Sullivan et al., 2020). However, further studies are needed to clarify the precipitation kinetics mainly driven by temperature.

The influence of pressure is even more complicated than that of temperature, especially when the pressure depletion approaches the bubble point. The solution loses the lighter gases, which significantly affects the equilibrium state of the crude oil (Chen et al., 2013; Hemmati-Sarapardeh et al., 2014; Wang et al., 2017). It can be said that overall, the influence of various factors on asphaltene deposition directly or indirectly affects the stability of crude oil.

The effects of interaction forces between asphaltene molecules (Silva et al., 2019; Ahmadi and Chen, 2020) and with inorganic solid particles (Nassar et al., 2015; Alimohammadi et al., 2019; Dashti et al., 2020; Nguyen et al., 2021) have also been researched using molecular dynamics studies. These studies are of great significance in understanding asphaltenes and improving resource recovery.

However, with the increasing demand for crude oil, the exploration and production of crude oil from unconventional reservoirs is inevitable (Elturki and Imqam, 2020; Simon et al., 2021). In the northwestern part of China, unconventional reserves have been identified characterized by ultra-depth (7000–12000 m), high-temperature (110–180 °C), high-pressure (75–150 MPa), and high gas-oil ratio (400–1000). The temperature and pressure drop gradients are extreme compared with conventional wells during production. Studies and field reports show that the risks associated with asphaltene deposition and plugging occur more frequently in these high-temperature/high-pressure (HTHP) wells than in conventional ones. Therefore, a comprehensive understanding of asphaltene behavior in high temperature and high-pressure conditions is vital in managing this problem.

The main objective of this paper is to study the various factors influencing asphaltene precipitation under HTHP reservoir conditions, i.e., temperature, pressure, gas-oil ratio, and analysis of the relationship between the gas-oil ratio. Moreover, an attempt is made at forecasting the onset of asphaltene precipitation in the wells using high pressure/high-temperature equipment.

2. Materials and methods

2.1. Materials

The crude oil T-A1 was obtained from the Tarim Oil Field (Xinjiang, China), and its properties are presented in Table 1. The CII value was calculated through SARA components of crude oil (CII value > 0.9 implies colloidal instability of crude oil) (Ashoori et al., 2017; Xiong et al., 2020b). Methane gas, 99.9% purity from Beijing Huatong Jingke Gas Chemical Co., Ltd was used.

2.2. Experimental apparatus

Fig. 1 is a schematic of the apparatus designed by the China University of Petroleum-Beijing to satisfy the ultra-deep, high-temperature, and high-pressure testing conditions. The device consists of two parts, namely a high-temperature, high-pressure PVT cell, and a Dynamic Light Scattering (DLS) system. The volume capacity of the PVT cell is 200 mL±0.001 mL. The DLS system includes the 90-W halogen lamp as a light source with a spectral range (200–1100 nm), optical fiber, signal detector, and data analysis system. Optic fiber transmits light from the light source to the sample, and a sensor collects the backscattered light. The optic fiber is attached on the PVT cell to keep the light paths fixed. The DLS system is operated in a dark environment to avoid the influence of ambient light.

Previous studies have shown that the dynamic light scattering method has a unique advantage in analyzing the behavior and growth of asphaltene particles under various experimental conditions (Yudin and Anisimov, 2007; Paridar et al., 2018; Shojaei et al., 2020). The Rayleigh and Debye theories are applied in this study to analyze the experimental results (Young and Lovell, 2011; Hiemenz and Rajagopalan, 2016).

2.3. Preparation of HTHP oil sample

Before testing, the system was vacuumed entirely. Pumping the crude oil sample into the PVT cell and re-exhausting with air treatment is necessary, according to the GOR 450 sm^3/sm^3 injected the methane gas. Consequently, the PVT cell is set to a temperature of 107.6 °C and a pressure of 97.98 MPa to mimic the reservoir conditions. During the process of making the HTHP oil sample, ultrasonic energy is provided to the sample to promote gas dissolution, and the PVT cell cylinder periodically is rotated between 45° and 270°. The whole sample mixing process lasts 48 h till the temperature and pressure are stabilized.

It is noted that after finishing the preparation of the HTHP oil sample, the PVT cell is turned upside down and left for 4 h. The primary purpose was to make the residual impurities, and any existing asphaltene particles in the crude fully settle and avoid their influence on the DLS measurements.

2.4. Experimental

2.4.1. Temperature effect

The air-cooling system tested the effect of temperature on the stability of crude oil, and the temperature was decreased from 107.6 °C to 33.5 °C, while the pressure remained stable. The testing process takes about 12 h, and the cell's volume, temperature, pressure are recorded by the PVT system every 10 s. The DLS system collects the backscattered light synchronized with the PVT system. Each measurement is repeated three times to ensure reproducibility.

2.4.2. Pressure effect

The isothermal depressurization method was used to analyze pressure's influence, and the same procedure was used as described in the previous section. The pressure depletion rate is set at 0.05 mL/min to avoid the scattering signal from being affected by gas bubbles produced when the pressure falls below the bubble point. In this work, the temperatures of 30 °C, 50 °C, 70 °C, 90 °C, 107.6 °C were tested, respectively. The HTHP oil sample needs to be

Table 1
Properties of oil sample.

Crude oil	Density, g/cm^3 (20 °C)	Saturates, wt%	Aromatics, wt%	Resins, wt%	Asphaltenes, wt%	CII Value
T-A1	0.8240	58.28	22.73	13.39	5.60	1.77

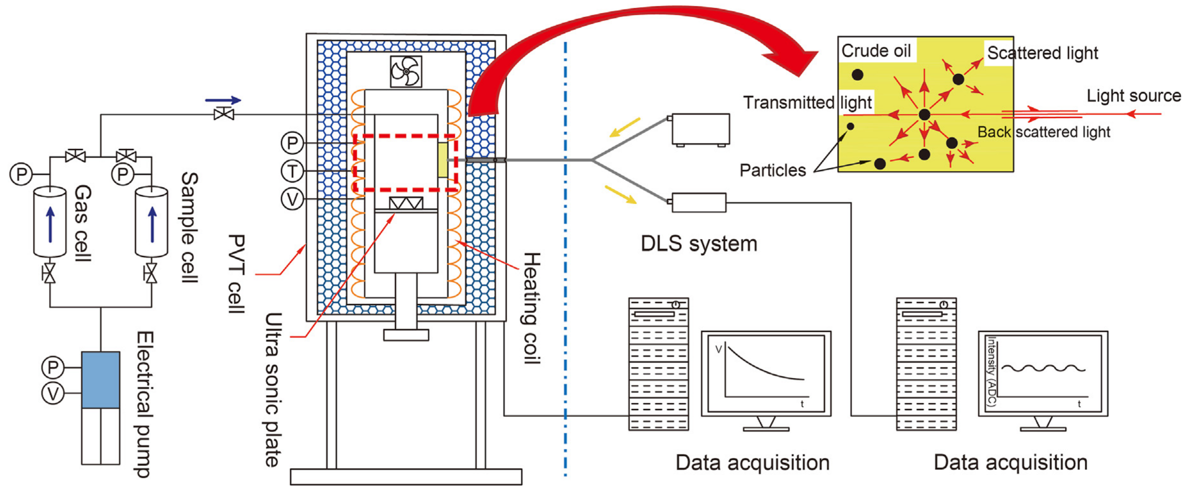

Fig. 1. Schematic of the high-temperature and high-pressure asphaltene analysis device. This device includes the high-temperature and high-pressure PVT cell (left) and the DLS system (right).

re-prepared as described before each time the test conditions are changed.

2.4.3. Gas-oil ratio (GOR) effect

This work tested GOR of 100 sm^3/sm^3, 200 sm^3/sm^3, 300 sm^3/sm^3 and 450 sm^3/sm^3 to analyze their influence on asphaltene deposition risk. Meanwhile, five temperature points (30 °C, 50 °C, 70 °C, 90 °C, 107.6 °C) were tested for each gas-oil ratio to determine the deposition envelope. The testing approach was the same as described in the sections above.

3. Results and discussion

3.1. Temperature effect on asphaltene precipitation

As seen in Fig. 2, the entire system is demarcated into three distinct regions based on the trend of the intensity curve, that is to say, 80–107 °C, 43–80 °C, and below 43 °C.

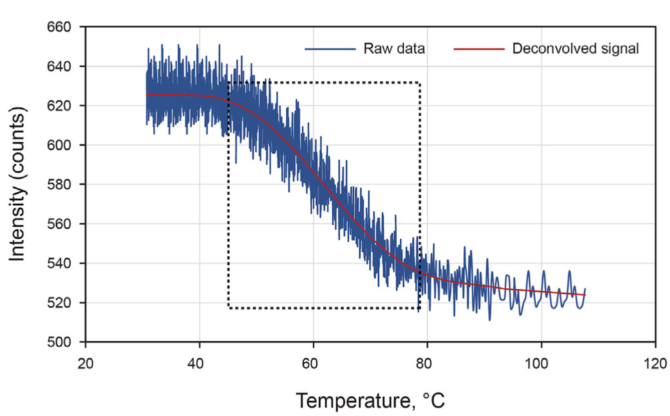

Fig. 2. Asphaltene precipitation plot of the backscattered light changes with temperature.

In the region above 80 °C, it is observed that the intensity is almost flat, signifying stability and uniformity (equilibrium state) for the overall system. Still, as the system's cooling continues below this region to 43 °C, there is a gradual increase in the intensity. The increase in this region has a linear dependence on the temperature decrease. This increase in the backscattered light indicates precipitation of solids in the system that continues up to 43 °C. In this case, it can be said that the asphaltene precipitation starts at about 80 °C and stops at about 43 °C. Below 43 °C, the curve flats out, implying the formation of a new stable colloidal system.

Further inspection of the temperature range (80–50 °C) reveals a linear dependence between the backscattered light intensity and the temperature. A regression analysis of this dependence shows that the data can be fitted to a linear model with a 86% correlation factor, Fig. 3.

The fitted model has a mean value of -3.106 ± 0.04 (counts/°C) with a P-value of 0.025 and ~98% confidence which implies that the mean is significantly meaningful.

Therefore, it can be said that a linear relation exists between colloids, causing the backscattering and the temperature. In this temperature range, the asphaltenes precipitate out of the fluid system.

3.2. Pressure effect on asphaltene precipitation

The pressure effect is tested at four different temperatures while maintaining the gas-oil ratio (Fig. 4). Although the inflexion points occur at different pressures, the overall dependence of the intensity on pressure depletion exhibits a similar trend at any given temperature. This implies that the general response of the system to pressure depletion is the same regardless of the temperature. Therefore, we can eliminate the temperature effect in this analysis and focus on the pressure effect. Fig. 4(a) shows that generally, at high pressure greater than 83 MPa, the intensity is stable. When pressure depletion is continued to 37.6 MPa, a gradual increase in intensity is observed from 83 MPa to 48 MPa, at which an inflexion

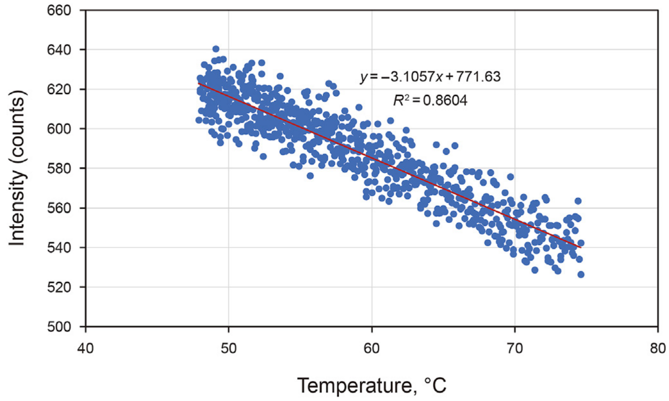

Fig. 3. Correlation of temperature and intensity (80–50 °C).

point is observed. At this pressure, maximum intensity is recorded before a sharp decrease in the intensity is registered between 48 and 37.6 MPa. Below 37.6 MPa, a slight increase in the intensity is observed before it flattens throughout.

As observed in Fig. 4(a), at high pressure (83–100 MPa), the intensity of the backscattered light is stable, because in this temperature range, the system is in an equilibrium state. The gradual increase below 83 MPa is attributed to the appearance of colloidal particles in the system that cause constructive interference (Hiemenz and Rajagopalan, 2016). The colloidal particles are asphaltenes precipitating out of the solution. At the inflexion point (48 MPa), the precipitation significantly slows down or ceases at most, and flocculation of the precipitants occurs. The flocculation causes an increase in particle size. Due to the big size of the particles (asphaltenes), destructive interference occurs, causing a sharp decrease in intensity before attaining a stable state. This state is a colloidal system comprising asphaltenes of different sizes and a fluid system. It is generally accepted that precipitation of asphaltenes ceases or completely slows down at the bubble point. Thus, we can deduce that the inflexion point is indeed the bubble point. Literature studies show two limits bound this point; upper asphaltene onset point (UOP) and lower asphaltene onset point (LOP). Therefore, from Fig. 4(a), the pressures of 83 MPa and 37.6 MPa correspond to these points.

3.3. Gas-oil ratio (GOR) effect on asphaltene precipitation

The contribution of GOR to asphaltene deposition risk is undisputed, and as observed in Fig. 5, high gas-oil ratios accelerate asphaltene precipitation. At a 450 sm^3/sm^3, the onset pressure is about 90 MPa compared to 32 MPa for a 100 sm^3/sm^3 gas-oil ratio. In investigating the impact of GOR on asphaltene behavior, we considered the inflexion point (Bubble point), the upper and lower asphaltene onset limits, and the maximum intensity at the inflexion point. In Fig. 6 are relationship plots of the dependence of the precipitation parameters on the gas-oil ratio.

It is observed that the onset points, inflexion point, and the intensity at the inflexion points can be fitted to a linear model. A

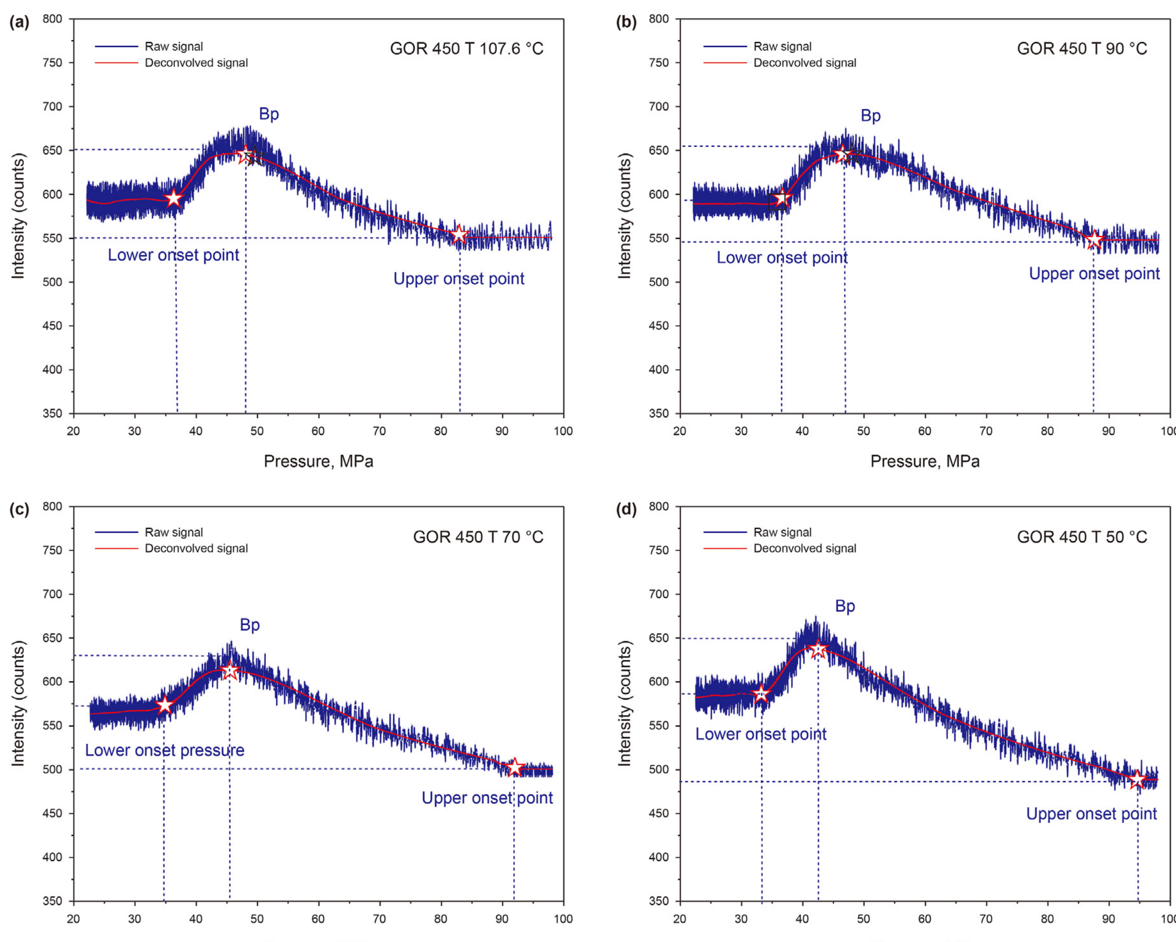

Fig. 4. Asphaltene precipitation plot of the backscattered light changes with pressure at various temperatures.

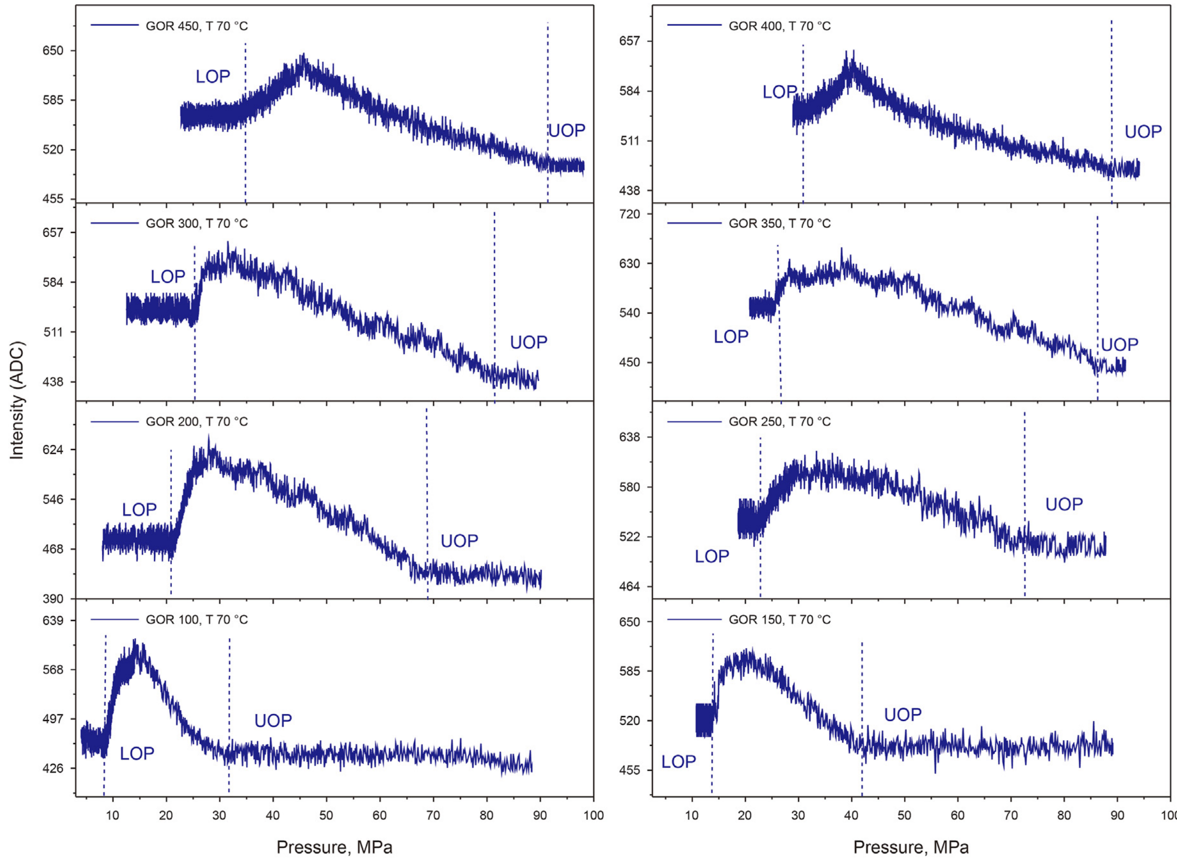

Fig. 5. Asphaltene appearance behavior under different gas-oil ratios (GOR).

regression analysis of the linear models reveals that models accurately predict the individual dependences of these parameters on the GOR (see appendix Fig. S1). Besides, from Table 2, by testing the hypothesis that the slope and intercept of the linear models are

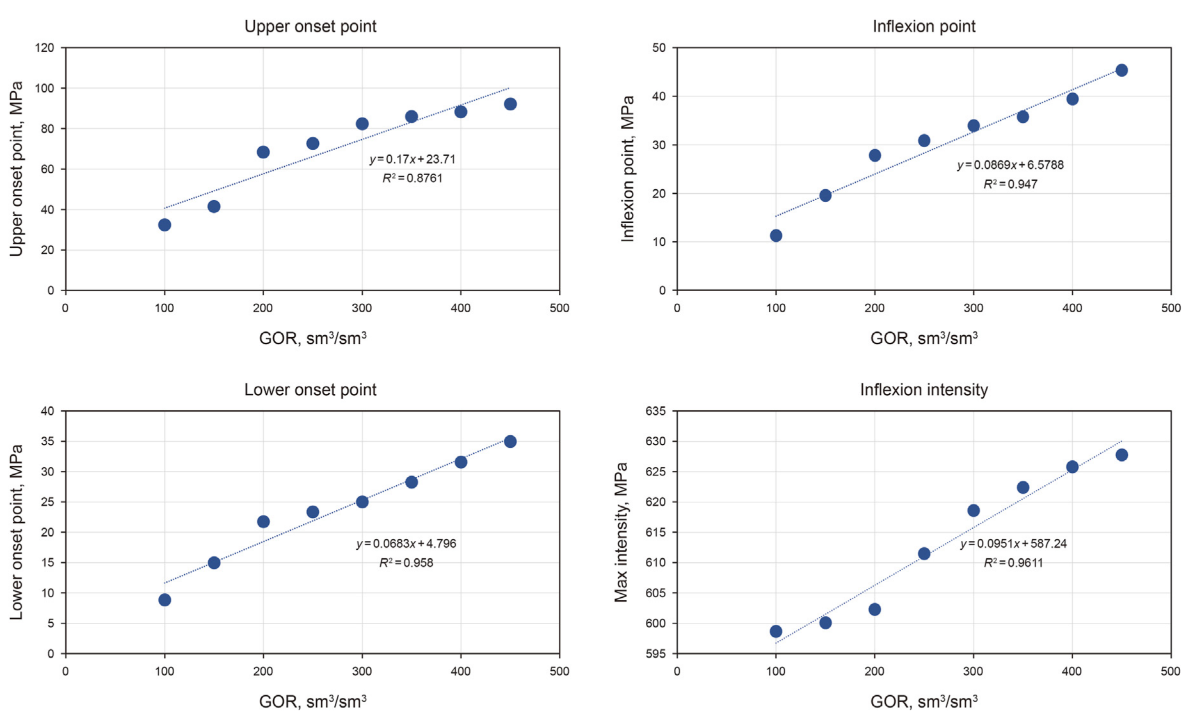

Fig. 6. Dependence of the precipitation parameters on the GOR.

Table 2
Summary of regression analysis on the parameters.

Parameters	Gradient	Standard error	P-value	Significance	Correlation coefficient
UOP	0.170	0.026	6×10^{-4}	99.9994	0.876
LOP	0.068	0.006	2×10^{-5}	100.0000	0.958
Inf.Point	0.087	0.008	5×10^{-5}	100.0000	0.947
Max.Int	0.095	0.008	2×10^{-5}	100.0000	0.961
Intercept					
UOP	23.710	7.775	2×10^{-2}	99.9775	0.876
LOP	4.796	1.741	3×10^{-2}	99.9669	0.958
Inf.Point	6.579	2.501	4×10^{-2}	99.9610	0.947
Max.Int	587.236	2.328	3×10^{-13}	100.0000	0.961

*Inf.Point-inflexion point, Max.Int-maximum intensity at inflexion point.

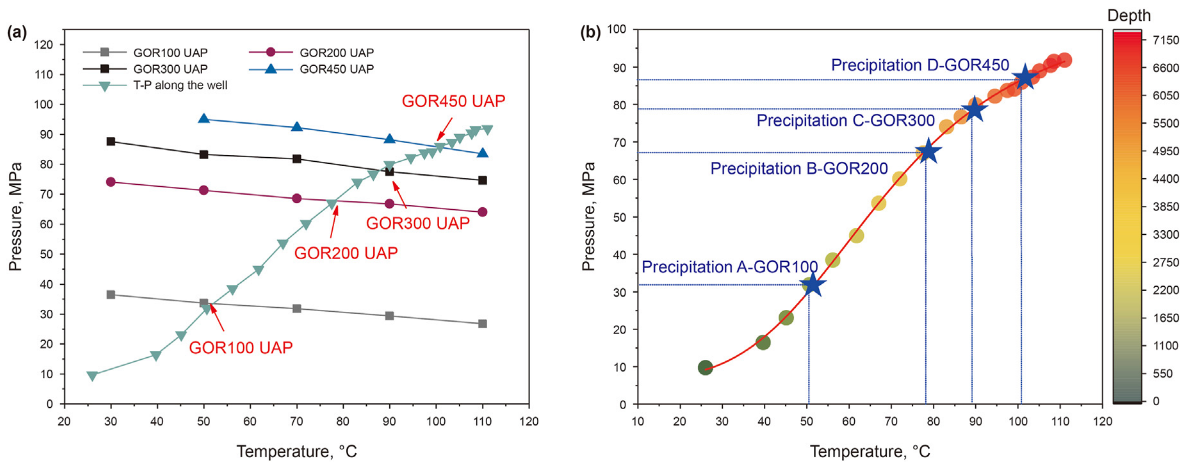

Fig. 7. Forecasting asphaltene onset in well TA-1 based on GOR. (**a**)Superposition of well T-P on the GOR curves. (**b**) Precipitation onset correlated with well depth.

generated from noise, it can be seen that the dependence of the parameters is meaningful. Besides, from the correlation coefficients, it is deduced that the parameters are correlated to the models by more than 85%. Therefore, the GOR has a significant effect on the asphaltenes' precipitation.

3.3.1. *Prediction of asphaltene risk in field well based on GOR*

Based on the simulated GOR experimental result, a pressure-temperature cross-plot is made to forecast asphaltene onset points along the HTHP well. As observed in Fig. 7(a), the temperature-pressure data is superimposed on the cross plot. At points where the simulated GOR intersects with the superimposed well data (see appendix), the temperature and pressure values at asphaltene precipitation onset expected in the well are determined. In Fig. 7(b), the onset temperature and pressure correlate with the well's depth, thus locating risk areas at each GOR.

A high GOR causes onsets in deeper sections of the well, while a low GOR causes onsets in shallow sections close to the surface. Armed with this knowledge, we can understand the risks posed by asphaltene deposition in HPHT wells used to remediate the impacts; for example, optimization of the nozzle opening to maintain control on GOR can be very useful.

4. Conclusion

This article investigates the influence of temperature, pressure, and gas-oil ratio of the HTHP oil reservoir. The following conclusions can be drawn:

(1) The temperature can change the solubility of asphaltene in crude oil. The effect of cooling on the behavior of asphaltene molecules in crude oil tends to accelerate asphaltene precipitation within a specific temperature range. The relationship in this range has been determined to be linear.
(2) The impacts of pressure and gas-oil ratio on the stability of crude oil colloidal system are more pronounced than that of temperature. The pressure depletion on crude with high asphaltene risk accelerates their precipitation, flocculation, and eventually deposition. At the pressures below the bubble point pressure, the precipitation is decelerated, and flocculation picks up. On the other hand, a high gas-oil ratio raises the upper asphaltene onset (UOP) points, whereas low GOR lower the UOP. It has also been determined that GOR has a linear impact on precipitation parameters assessed in this study.

Credit Author Statement

Rui-Ying Xiong: Conceptualization, Investigation; Data curation; Methodology; Writing-Draft. Ji-Xiang Guo: Funding acquisition; and Supervision. Wyclif Kiyingi: Conceptualization, Methodology; Analysis, Writing & Review. Hai-Xia Xu: Field application guiding; Data curation. Xin-Peng Wu: Experimentation.

Declaration of conflict of interest

There are no conflicts of interest needed to be declared in this manuscript.

Acknowledgment

The authors would like to thank Professor Savvas G. Hatzikiriakos (University of British Columbia) for his helpful advice on improving our work.

This work was supported by the National Natural Science Foundation of China (No. 52174047), and the China Scholarship Council (No. 202106440102), and the PetroChina Strategic Cooperation Science and Technology Project (No. ZLZX 2020-01).

Appendix A. Supplementary data

Supplementary data to this article can be found online at https://doi.org/10.1016/j.petsci.2022.08.026.

References

Ahmadi, M., Chen, Z., 2020. Insight into the interfacial behavior of surfactants and asphaltenes: molecular dynamics simulation study. Energy Fuel. 34 (11), 13536–13551. https://doi.org/10.1021/acs.energyfuels.0c01596.

Alimohammadi, S., Zendehboudi, S., James, L., 2019. A comprehensive review of asphaltene deposition in petroleum reservoirs: theory, challenges, and tips. Fuel 252, 753–791. https://doi.org/10.1016/j.fuel.2019.03.016.

Alqam, M.H., Abu-Khamsin, S.A., Sultan, A.S., Al-Afnan, S.F., Alawani, N.A., 2021. An investigation of factors influencing carbonate rock wettability. Energy Rep. 7, 1125–1132. https://doi.org/10.1016/j.egyr.2021.01.091.

Ashoori, S., Sharifi, M., Masoumi, M., Salehi, M.M., 2017. The relationship between SARA fractions and crude oil stability. Egypt. J. Petrol. 26 (1), 209–213. https://doi.org/10.1016/j.ejpe.2016.04.002.

Bahrami, P., Kharrat, R., Mahdavi, S., Firoozinia, H., 2015. Prediction of the gas injection effect on the asphaltene phase envelope. Oil Gas Sci. Technol. Revue d'IFP Energies nouvelles 70 (6), 1075–1086. https://doi.org/10.2516/ogst/2014037.

Balestrin, L.B.S., Cardoso, M.B., Loh, W., 2017. Using atomic force microscopy to detect asphaltene colloidal particles in crude oils. Energy Fuel. 31 (4), 3738–3746. https://doi.org/10.1021/acs.energyfuels.6b03333.

Chen, C., Guo, J., An, N., Ren, B., Li, Y., Jiang, Q., 2013. Study of asphaltene deposition from Tahe crude oil. Petrol. Sci. 10 (1), 134–138. https://doi.org/10.1007/s12182-013-0260-y.

Dashti, H., Zanganeh, P., Kord, S., Ayatollahi, S., Amiri, A., 2020. Mechanistic study to investigate the effects of different gas injection scenarios on the rate of asphaltene deposition: an experimental approach. Fuel 262, 116615. https://doi.org/10.1016/j.fuel.2019.116615.

Dutta Majumdar, R., Bake, K.D., Ratna, Y., Pomerantz, A.E., Mullins, O.C., Gerken, M., Hazendonk, P., 2016. Single-core PAHs in petroleum-and coal-derived asphaltenes: size and distribution from solid-state NMR spectroscopy and optical absorption measurements. Energy Fuel. 30 (9), 6892–6906. https://doi.org/10.1021/acs.energyfuels.5b02815.

Elturki, M., Imqam, A., 2020. High pressure-high temperature nitrogen interaction with crude oil and its impact on asphaltene deposition in nano shale pore structure: an experimental study. SPE/AAPG/SEG Unconventional Resources Technology Conference. OnePetro. https://doi.org/10.15530/urtec-2020-3241.

Fakher, S., Ahdaya, M., Elturki, M., Imqam, A., 2020. Critical review of asphaltene properties and factors impacting its stability in crude oil. J. Pet. Explor. Prod. Technol. 10 (3), 1183–1200. https://doi.org/10.1007/s13202-019-00811-5.

Ghadimi, M., Amani, M.J., Ghaedi, M., Malayeri, M.R., 2019. Modeling of formation damage due to asphaltene deposition in near wellbore region using a cylindrical compositional simulator. J. Petrol. Sci. Eng. 173, 630–639. https://doi.org/10.1016/j.petrol.2018.10.058.

Goual, L., Sedghi, M., Mostowfi, F., McFarlane, R., Pomerantz, A.E., Saraji, S., Mullins, O.C., 2014. Cluster of asphaltene nanoaggregates by DC conductivity and centrifugation. Energy Fuel. 28 (8), 5002–5013. https://doi.org/10.1021/ef5010682.

Guzmán, R., Ancheyta, J., Trejo, F., Rodríguez, S., 2017. Methods for determining asphaltene stability in crude oils. Fuel 188, 530–543. https://doi.org/10.1016/j.fuel.2016.10.012.

Guzmán, R., Rodríguez, S., Torres-Mancera, P., Ancheyta, J., 2020. Evaluation of asphaltene stability of a wide range of Mexican crude oils. Energy Fuel. 35 (1), 408–418. https://doi.org/10.1021/acs.energyfuels.0c03301.

Hemmati-Sarapardeh, A., Ahmadi, M., Ameli, F., Dabir, B., Mohammadi, A.H., Husein, M.M., 2019. Modeling asphaltene precipitation during natural depletion of reservoirs and evaluating screening criteria for stability of crude oils. J. Petrol. Sci. Eng. 181, 106127. https://doi.org/10.1016/j.petrol.2019.05.078.

Hemmati-Sarapardeh, A., Ayatollahi, S., Zolghadr, A., Ghazanfari, M.H., Masihi, M., 2014. Experimental determination of equilibrium interfacial tension for nitrogen-crude oil during the gas injection process: the role of temperature, pressure, and composition. J. Chem. Eng. Data 59 (11), 3461–3469. https://doi.org/10.1021/je5004274.

Hiemenz, P.C., Rajagopalan, R., 2016. Principles of Colloid and Surface Chemistry, Revised and Expanded. CRC press. https://doi.org/10.1201/9781315274287.

Hu, Y.F., Guo, T.M., 2001. Effect of temperature and molecular weight of nalkane precipitants on asphaltene precipitation. Fluid Phase Equil. 192 (1–2), 13–25. https://doi.org/10.1016/S0378-3812(01)00619-7.

Lei, Y., Han, S., Zhang, J., 2016. Effect of the dispersion degree of asphaltene on wax deposition in crude oil under static conditions. Fuel Process. Technol. 146, 20–28. https://doi.org/10.1016/j.fuproc.2016.02.005.

Mohammed, I., Mahmoud, M., Al Shehri, D., El-Husseiny, A., Alade, O., 2020. Asphaltene precipitation and deposition: a critical review. J. Petrol. Sci. Eng. 197, 107956. https://doi.org/10.1016/j.petrol.2020.107956.

Mousavi, M., Abdollahi, T., Pahlavan, F., Fini, E.H., 2016. The influence of asphaltene-resin molecular interactions on the colloidal stability of crude oil. Fuel 183, 262–271. https://doi.org/10.1016/j.fuel.2016.06.100.

Mullins, O.C., 2010. The modified Yen model. Energy Fuel. 24 (4), 2179–2207. https://doi.org/10.1021/ef900975e.

Mullins, O.C., Sabbah, H., Eyssautier, J., Pomerantz, A.E., Barré, L., Andrews, A.B., Ruiz-Morales, Y., Mostowfi, F., McFarlane, R., Goual, L., Lepkowicz, R., Cooper, T., Orbulescu, J., Leblanc, R.M., Edwards, J., Zare, R.N., 2012. Advances in asphaltene science and the Yen–Mullins model. Energy Fuel. 26 (7), 3986–4003. https://doi.org/10.1021/ef300185p.

Nassar, N.N., Betancur, S., Acevedo, S.C., Franco, C.A., Cortés, F.B., 2015. Development of a population balance model to describe the influence of shear and nanoparticles on the aggregation and fragmentation of asphaltene aggregates. Ind. Eng. Chem. Res. 54 (33), 8201–8211. https://doi.org/10.1021/acs.iecr.5b02075.

Nguele, R., Poupi, A.B.M., Anombogo, G.A.M., Alade, O.S., Saibi, H., 2022. Influence of asphaltene structural parameters on solubility. Fuel 311, 122559. https://doi.org/10.1016/j.fuel.2021.122559.

Nguyen, D.D., Daneshfar, R., Dehaghani, A.H.S., Su, C.H., 2021. The effect of shear rate on aggregation and breakage of asphaltenes flocs: experimental study and model-based analysis. J. Mol. Liq. 325, 114861. https://doi.org/10.1016/j.molliq.2020.114861.

Paridar, S., Nazar, A.R.S., Karimi, Y., 2018. Experimental evaluation of asphaltene dispersants performance using dynamic light scattering. J. Petrol. Sci. Eng. 163, 570–575. https://doi.org/10.1016/j.petrol.2018.01.013.

Raljević, D., Vuković, J.P., Smrečki, V., Pajc, L.M., Novak, P., Hrenar, T., Jednačak, T., Konjević, L., Pinević, B., Gašparac, T., 2021. Machine learning approach for predicting crude oil stability based on NMR spectroscopy. Fuel 305, 121561. https://doi.org/10.1016/j.fuel.2021.121561.

Schuler, B., Meyer, G., Peña, D., Mullins, O.C., Gross, L., 2015. Unraveling the molecular structures of asphaltenes by atomic force microscopy. J. Am. Chem. Soc. 137 (31), 9870–9876. https://doi.org/10.1021/jacs.5b04056.

Shojaei, S.A., Osfouri, S., Azin, R., Dehghani, S.A.M., 2020. Kinetic modeling of asphaltene nano-aggregates formation using dynamic light scattering technique. J. Petrol. Sci. Eng. 192, 107293. https://doi.org/10.1016/j.petrol.2020.107293.

Siddiqui, M.A., Tariq, S.M., Haneef, J., Ali, S.I., Manzoor, A.A., 2019. Asphaltene stability analysis for crude oils and their relationship with asphaltene precipitation models for a gas condensate field. SPE Middle East Oil and Gas Show and Conference. OnePetro. https://doi.org/10.2118/194706-MS.

Silva, H.S., Alfarra, A., Vallverdu, G., Bégué, D., Bouyssiere, B., Baraille, I., 2019. Asphaltene aggregation studied by molecular dynamics simulations: role of the molecular architecture and solvents on the supramolecular or colloidal behavior. Petrol. Sci. 16 (3), 669–684. https://doi.org/10.1007/s12182-019-0321-y.

Simon, R.E., Johnson, S.C., Khatib, O., Raschke, M.B., Budd, D.A., 2021. Correlative nano-spectroscopic imaging of heterogeneity in migrated petroleum in unconventional reservoir pores. Fuel 300, 120836. https://doi.org/10.1016/j.fuel.2021.120836.

Sinnathamb, C.M., Nor, N.M., 2012. Relationship between SARA fractions and crude oil fouling. J. Appl. Sci. 12 (23), 2479–2483. https://doi.org/10.3923/jas.2012.2479.2483.

Sullivan, M., Smythe, E., Fukagawa, S., Harrison, C., Dumont, H., Borman, C., 2020. A fast measurement of asphaltene onset pressure. SPE Reservoir Eval. Eng. 23 (3), 962–978. https://doi.org/10.2118/199900-PA.

Wang, J., Bai, Y., Sui, H., Li, X., He, L., 2021. Understanding the effects of salinity on bitumen-calcite interactions. Fuel Process. Technol. 213, 106668. https://doi.org/10.1016/j.fuproc.2020.106668.

Wang, Z., Xu, J., Liu, H., Hou, J., Zhang, Y., 2017. Effect of pressure, temperature, and mass fraction of CO_2 on the stability of the asphaltene constituents in crude oil. Petrol. Sci. Technol. 35 (22), 2109–2114. https://doi.org/10.1080/10916466.2017.1384838.

Xiong, Q.Y., Kiyingi, W., Pan, J.J., Xiong, R.Y., Deng, W., Zhang, S.L., Guo, J.X., Yang, Y.Q., 2020a. Analysis of Xinjiang asphaltenes using high precision spectroscopy. RSC Adv. 10 (65), 39425–39433. https://doi.org/10.1039/D0RA07278H.

Xiong, R.Y., Guo, J.X., Kiyingi, W., Feng, H.S., Sun, T.C., Yang, X.H., Li, Q., 2020b. Method for judging the stability of asphaltenes in crude oil. ACS Omega 5 (34), 21420–21427. https://doi.org/10.1021/acsomega.0c01779.

Yao, B., Chen, W., Li, C.X., Yang, F., Sun, G.Y., Wang, G.Y., Xu, H.C., 2020. Polar asphaltenes facilitate the flow improving performance of polyethylene-vinyl acetate. Fuel Process. Technol. 207, 106481. https://doi.org/10.1016/j.fuproc.2020.106481.

Yarranton, H.W., 2005. Asphaltene self-association. J. Dispersion Sci. Technol. 26 (1),

5–8. https://doi.org/10.1081/DIS-200040234.
Young, R.J., Lovell, P.A., 2011. Introduction to Polymers. CRC press. https://doi.org/10.1201/9781439894156.
Yudin, I.K., Anisimov, M.A., 2007. Dynamic light scattering monitoring of asphaltene aggregation in crude oils and hydrocarbon solutions. In: Asphaltenes, Heavy Oils, and Petroleomics. Springer, pp. 439–468. https://doi.org/10.1007/0-387-68903-6_17.
Zuo, J.Y., Elshahawi, H., Mullins, O.C., Dong, C., Zhang, D., Jia, N., Zhao, H.Y., 2012. Asphaltene gradients and tar mat formation in reservoirs under active gas charging. Fluid Phase Equil. 315, 91–98. https://doi.org/10.1016/j.fluid.2011.11.024.
Zuo, J.Y., Pan, S., Wang, K., Mullins, O.C., Dumont, H., Chen, L., Mishra, V., Canas, J., 2017. Analysis of asphaltene instability using diffusive and thermodynamic models during gas charges into oil reservoirs. Energy Fuel. 31 (4), 3717–3728. https://doi.org/10.1021/acs.energyfuels.6b03305.